Graphical Abstract

A Comparative Study of Identification Methods for Structural Dynamics: Evaluating DMD, DNN, and FEDNN

Alejandro Díaz

Highlights

A Comparative Study of Identification Methods for Structural Dynamics: Evaluating DMD, DNN, and FEDNN

Alejandro Díaz

- Research highlight 1
- Research highlight 2

A Comparative Study of Identification Methods for Structural Dynamics: Evaluating DMD, DNN, and FEDNN

Alejandro Díaz

[a]*Cinvestav, , Zapopan, 45069, Jalisco, Mexico*

Abstract

This paper presents a comparison of three identification methods. A cantilever beam was equipped with multiple sensors and subjected to an impulse. Sensor data, including positions and velocities, was captured using a MoCap system and utilized for parameter identification of the system without prior knowledge of its dynamics. The objective of this study is to compare three distinct identification methods: Dynamic Mode Decomposition (DMD), a basic Differential Neural Network (DNN), and a Finite Element Differential Neural Network (FEDNN) as introduced in [1]. Each method will be evaluated in terms of error, computational weight, and training challenges.

Keywords:
DMD, DNN, FEDNN, Cantilever Beam, Comparison

1. Introduction

When discussing identification methods, there exists a broad range of techniques that can be implemented [2]. Some of these methods require prior information from the system, which may not always be readily available. Furthermore, approaches such as the Finite Element Method (FEM) can account for deformities or additional elements such as actuators. Consequently, data-driven techniques can be particularly implemented for mathematical models involving Partial Differential Equations (PDE) [3].

The specific structure under consideration in this paper is precisely modeled as a Partial Differential Equation (PDE). This flexible structure, known as a cantilever beam, represents a distributed parameter system with an in-finite number of vibration modes [4]. It is regarded as a continuous system because each point within it can vibrate.

The cantilever beam is an extensively studied structure, widely employed across various fields including robotics, aerospace technology, and construction, among others [5]. For instance, rotating blades are often idealized as cantilever beams [6]. Consequently, numerous identification strategies have been implemented to model such systems, with the FEM being a prominent approach [7]. However, despite its widespread use, FEM exhibits low computational efficiency and cannot ensure continuous second derivatives at the element nodes [8]. Furthermore, these approaches typically rely on obtaining certain information from the system under analysis. However, in real-world scenarios, obtaining comprehensive system information may not always be feasible.

This limitation has led to the exploration of alternative identification techniques that rely solely on experimental data. It is necessary to mention, while the data for this study were collected from a cantilever beam due to its simplicity, the comparative analysis presented in this paper is applicable to a wide range of systems for which experimental data can be acquired[9].

This paper presents a comparative analysis of three different identification methods, comprising two neural network-based approaches and an experimental analysis utilizing the best linear fit method known as Dynamic Mode Decomposition (DMD). Each of these techniques is described in section 2.The remaining sections of the paper present the results in Section 3, and the conclusions in Section 4

The overall objective of this work is to demonstrate the differences in time and hardware resources required for identification based on real data acquired through a Motion Capture system (MoCap).

2. Methodology

The experimental setup for obtaining the measurement data involved the utilization of a MoCap system to directly record the positions and velocities of an aluminum beam. The beam was instrumented with twenty equidistant marks and fixed at one end, therefore, a cantilever beam. Subsequently, an impulse force was applied at the tenth node. The system response was recorded at a frequency of 100 Hz, which is the maximum frequency the MoCap is capable.

Each identification method explained in this section was implemented through Matlab code, and subsequently executed using the real data acquired from the MoCap.

For both the DNN and FEDNN methods, the same Finite Element Method (FEM) code was employed to calculate the stiffness matrix required for both techniques. Each method was individually fine-tuned, this process implies a significant change in the difficulty of the training process. Overall, The details of this comparison will be discussed in Section 3.

2.1. Dynamic Mode Decomposition (DMD)

The DMD technique has emerged as a powerful tool for analyzing the dynamics of nonlinear systems [10]. The workings of this method are detailed in [11]; however, we provide a brief explanation here, specially we remark that DMD utilizes data collected directly from the plant to identify the best linear fit that models its dynamics.

The idea behind this method is to have a time series of collected data. Each of these time stamps will be referred to as snapshots throughout this paper. The measurements, xk and $xk + 1$, where k stands for a temporary iteration, are assumed to be related through a linear operator, as shown in Equation (1).

$$x_{k+1} = Ax_k \tag{1}$$

Under this assumption, we proceed to organize our data into long vectors, each containing all the measurements from our states in that specific time interval, represented by matrix

$$X = \begin{bmatrix} | & | & & | \\ x_1 & x_2 & \cdots & x_{m-1} \\ | & | & & | \end{bmatrix} \subset \mathbb{R}^{nxt} \tag{2}$$

where n is the number of measured states and t the snapshot collected minus one.

Also, we form the matrix

$$X' = \begin{bmatrix} | & | & & | \\ x_2 & x_3 & \cdots & x_m \\ | & | & & | \end{bmatrix} \subset \mathbb{R}^{nxt} \tag{3}$$

Therefore, the relationship described in Equation (1) can be interpreted as

$$X' \approx AX \tag{4}$$

The primary objective of DMD is to solve for an approximation of the process matrix A for the measurement matrix pair X and X'.

Of course, it is possible to consider the impulse as an input signal. It is assumed that we can measure this input signal simultaneously with the states, and thus form the matrix

$$\Upsilon = \begin{bmatrix} | & | & & | \\ u_1 & u_2 & \cdots & u_{m-1} \\ | & | & & | \end{bmatrix} \subset \mathbb{R}^{nxt} \tag{5}$$

modifying the relationship to

$$X' \approx AX + B\Upsilon \tag{6}$$

Given this, we are presented with two possible cases. **Case 1** assumes that we know the value of B, implying that we have information about how the input affects the system. In this case, we can easily form

$$X' - B\Upsilon \approx AX \tag{7}$$

and find the value of A through the DMD algorithm.

To explore this possibility, a FEM Matlab code was utilized [12] to derive an estimated B.

Additionally, the **Case 2** of DMD method, where all parameters are unknown, was also implemented. For this case, we form the system as

$$X' \approx G\Omega \tag{8}$$

where $G = [A\ B]$ and $\Omega = [X\ \Upsilon]^T$. And proceed to find G.

Both cases are presented and compared in section 3.

2.2. Differential Neural Network (DNN)

For de DNN identification, we use the following neural network structure:

$$\dot{\hat{x}} = A\hat{x}_t + W_{1,t}\sigma(\hat{x}_t) + W_{2,t}\phi(\hat{x}_t)\gamma(u_t) \tag{9}$$

where

We assume that there exist weight matrices W_1^* and W_2^* such that the given system can be completely presented by

$$\dot{\hat{x}} = A\hat{x}_t + W_1^*\sigma(\hat{x}_t) + W_2^*\phi(\hat{x}_t)\gamma(u_t)$$

Under the following assumptions

Assumption 1. *The function $\phi(.)$ and $\sigma(.)$ satisfy sector condition []*

Assumption 2. *The nonlinear function $\gamma(.)$ is selected as*

$$\|\gamma(u_t)\|^2 \leq \bar{u}$$

There exist two possibilities to fulfill this constraint:

- *Consider bounder $\gamma(.)$ function*
- *Use bounded control actions $\{u_t\}(\|u_t\| \leq u^+ < \infty)$ and assume that the nonlinearity $\gamma(.)$ is continuous.*

Assumption 3. *There exist a strictly positive defined matrix Q_0 such that for*

$$R := \bar{W}_1 + \bar{W}_2$$

and

$$Q := Q_0 + D_\sigma + D_\phi \bar{u}$$

the matrix Riccati equation has a positive solution.

The weight adjusted law:

$$\dot{W}_{1,t} = -K_1 P \Delta_t \sigma(\hat{x}_t)^T \quad (10)$$

$$\dot{W}_{2,t} = -K_2 P \Delta_t \gamma(u_t)^T \phi(\hat{x}_t)^T \quad (11)$$

with $W_{1,0}, W_{2,0}$ being the initial weight matrices, K_1 and K_2 are positive defined matrices and P is the solution of matrix Ricatti Equation, then our network converges to the real system [13].

2.3. Finite Element Differential Neural Network (FEDNN)

For the FEDNN we use the next structure:

$$\dot{x} \quad (12)$$

[1]

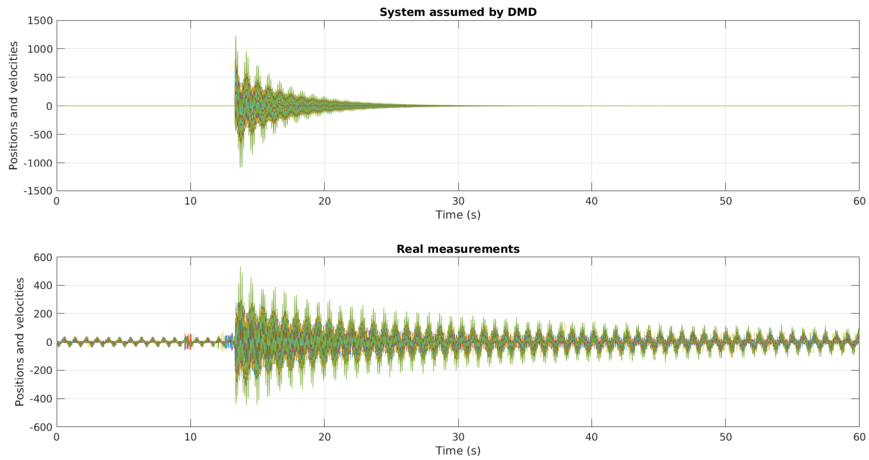

Figure 1: All nodes position and velocities (above) predicted by the DMD technique (below) measured by de MoCap

3. Experimental Results

Figure 1 presents a comparison between the system predicted by the DMD method and the real system subjected to the same impulse at the same node. Figure 2 illustrates the average error over time between both systems. Clearly, the maximum error occurs precisely at the moment the impulse is applied to the system. As depicted in Figure 2, this error gradually tends asymptotically to zero before the impulse is introduced. This condition tends to be similar for both cases, whether B is known or unknown. The plot for the second case (see Figure 3) reveals a noticeable difference between the predicted system and the real measurements. However, upon examination of Figure 4, it becomes apparent that this difference is actually less pronounced than in the first case.

4. Conclusions

5. Discussion

Appendix A. Example Appendix Section

Appendix text.

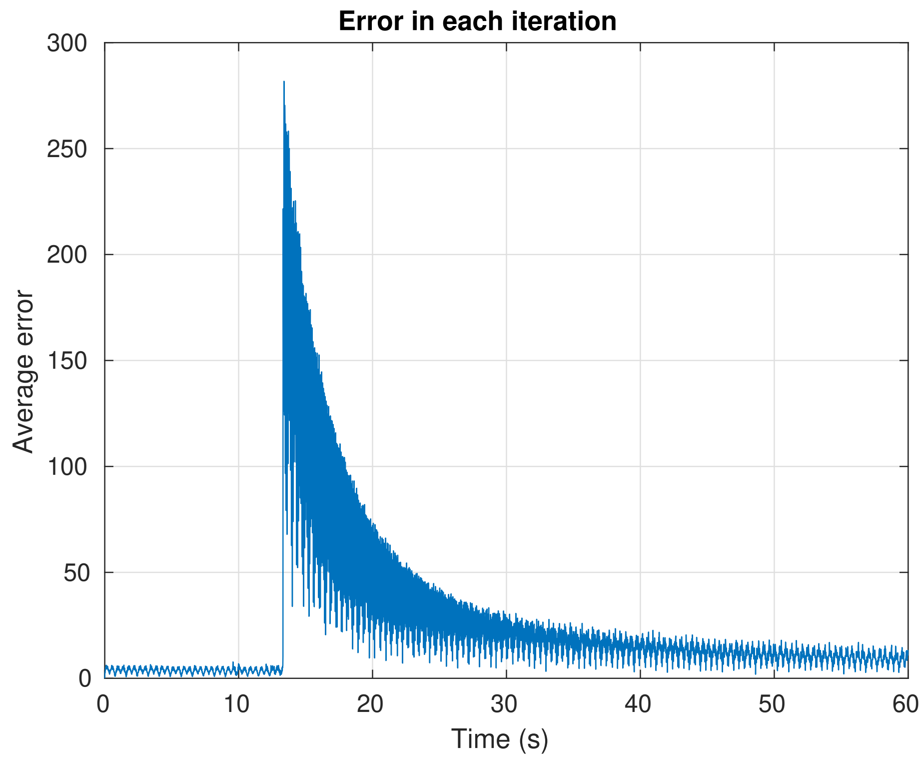

Figure 2: Average error

References

[1] O. Aguilar-Leal, R. Q. Fuentes-Aguilar, I. Chairez, A. García-González, J. C. Huegel, Distributed parameter system identification using finite element differential neural networks, Applied Soft Computing 43 (2016) 633–642.

[2] E. Reynders, System identification methods for (operational) modal analysis: review and comparison, Archives of Computational Methods in Engineering 19 (2012) 51–124.

[3] S. Rudy, A. Alla, S. L. Brunton, J. N. Kutz, Data-driven identification of parametric partial differential equations, SIAM Journal on Applied Dynamical Systems 18 (2) (2019) 643–660.

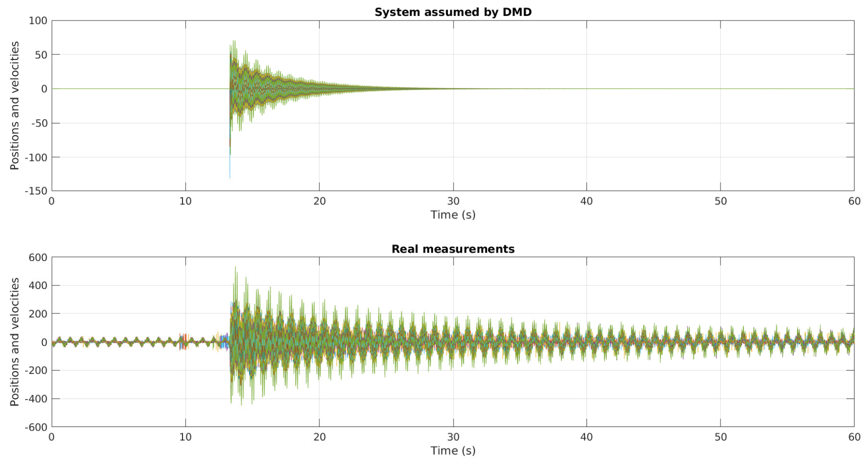

Figure 3: Figure Caption

[4] P.-T. Pham, K.-S. Hong, Dynamic models of axially moving systems: A review, Nonlinear Dynamics 100 (1) (2020) 315–349.

[5] P.-T. Pham, G.-H. Kim, Q. C. Nguyen, K.-S. Hong, Control of a non-uniform flexible beam: Identification of first two modes, International Journal of Control, Automation and Systems 19 (11) (2021) 3698–3707.

[6] T. Yokoyama, Free vibration characteristics of rotating timoshenko beams, International Journal of Mechanical Sciences 30 (10) (1988) 743–755.

[7] O. Garcia-Perez, G. Silva-Navarro, J. Peza-Solis, Flexible-link robots with combined trajectory tracking and vibration control, Applied Mathematical Modelling 70 (2019) 285–298.

[8] J. Fan, D. Zhang, H. Shen, Dynamic modeling and simulation of a rotating flexible hub-beam based on different discretization methods of deformation fields, Archive of Applied Mechanics 90 (2020) 291–304.

[9] J. C. Bello-Robles, O. Begovich, J. Ruiz-León, R. Q. Fuentes-Aguilar, Modeling of the temperature distribution of a greenhouse using finite element differential neural networks, Kybernetika 54 (5) (2018) 1033–1048.

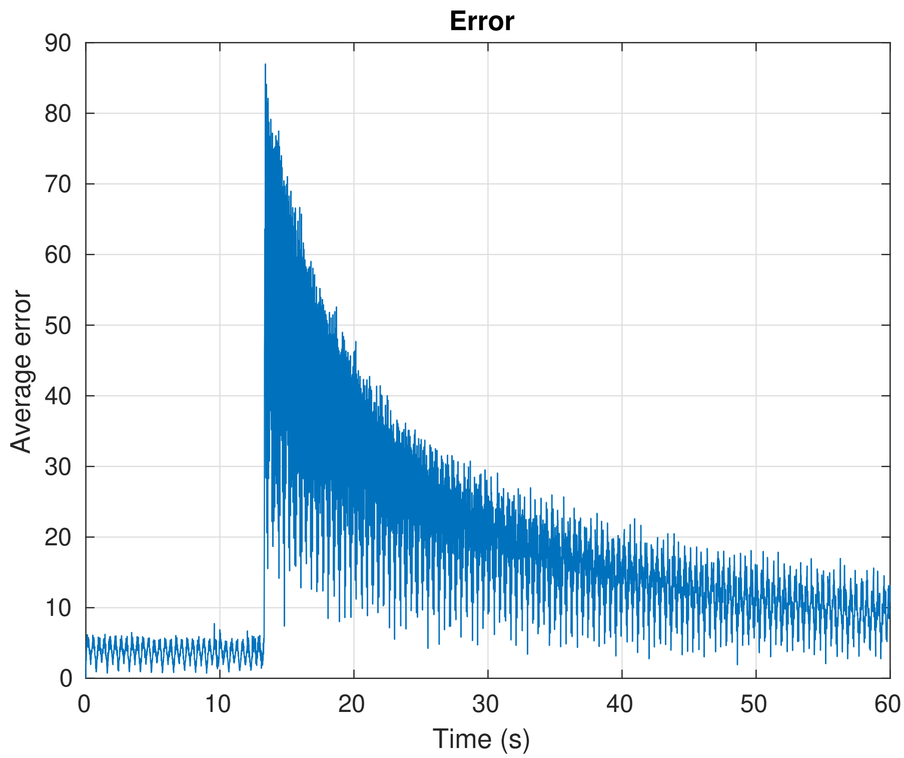

Figure 4: Figure Caption

[10] J. H. Tu, Dynamic mode decomposition: Theory and applications, Ph.D. thesis, Princeton University (2013).

[11] J. L. Proctor, S. L. Brunton, J. N. Kutz, Dynamic mode decomposition with control, SIAM Journal on Applied Dynamical Systems 15 (1) (2016) 142–161.

[12] Y. W. Kwon, H. Bang, The finite element method using MATLAB, CRC press, 2018.

[13] A. S. Poznyak, E. N. Sanchez, W. Yu, Differential neural networks for robust nonlinear control: identification, state estimation and trajectory tracking, World Scientific, 2001.

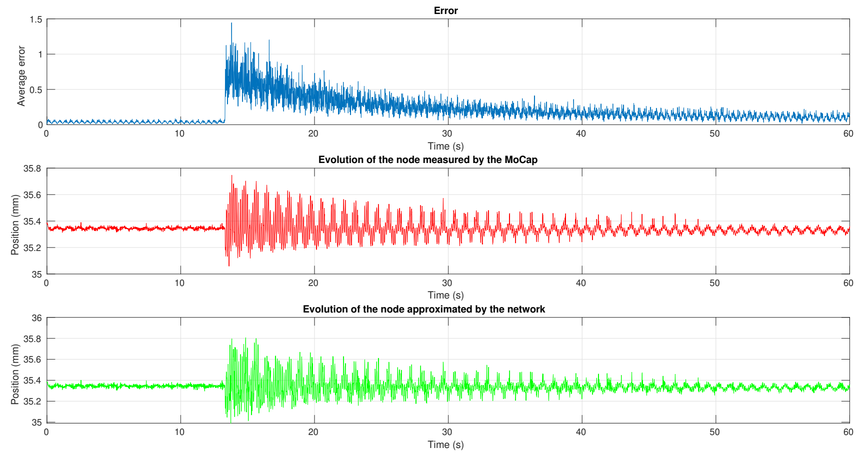

Figure 5: Figure Caption

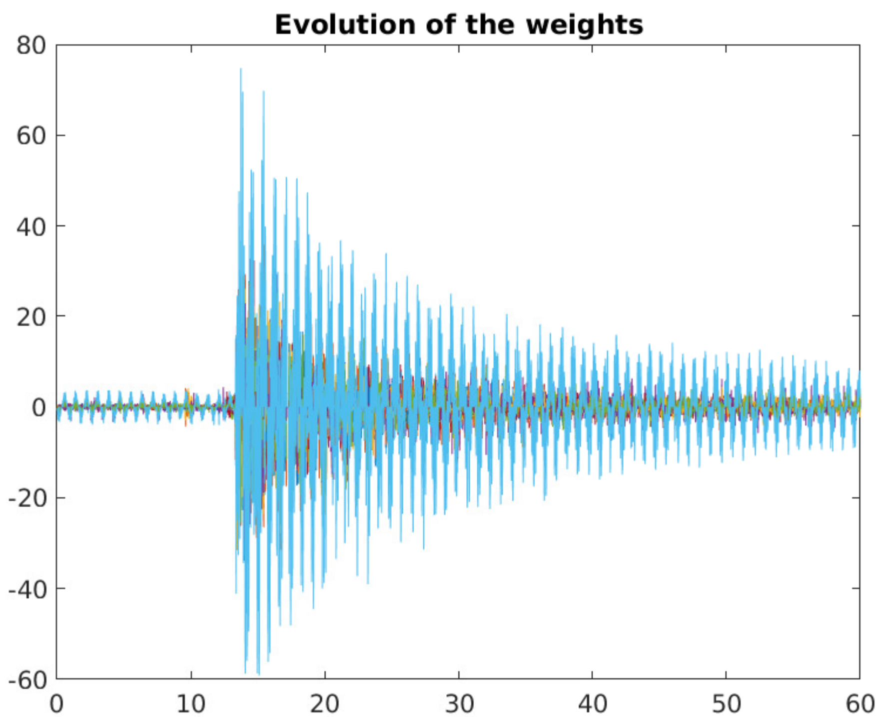

Figure 6: Figure Caption

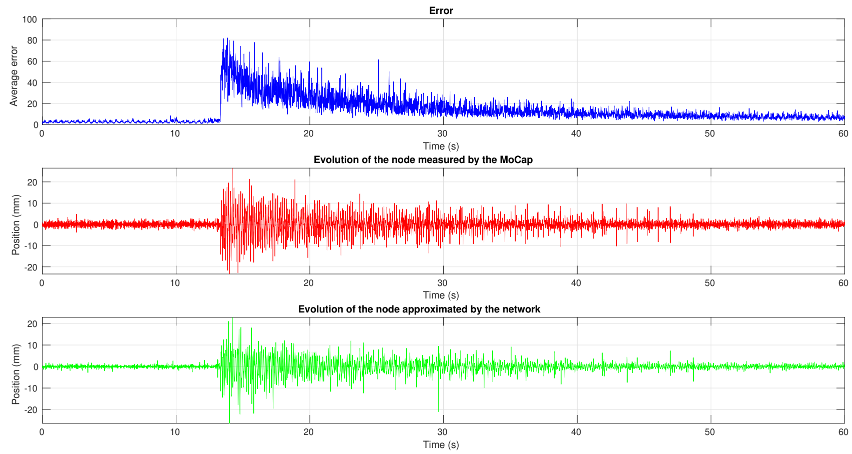

Figure 7: Figure Caption

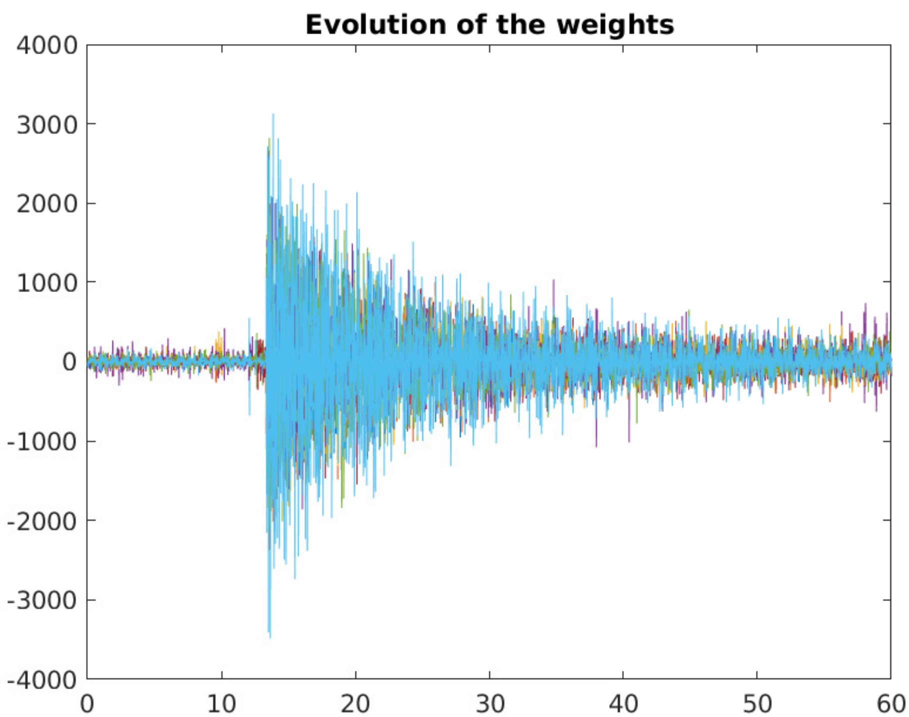

Figure 8: Figure Caption